Tumor Biology and Immunology

Cancer Research

Metformin-Induced Reduction of CD39 and CD73 Blocks Myeloid-Derived Suppressor Cell Activity in Patients with Ovarian Cancer

Lifeng Li[1,2], Liping Wang[2], Jieyao Li[2], Zhirui Fan[2], Li Yang[1], Zhen Zhang[1,2], Chaoqi Zhang[1,2], Dongli Yue[2], Guohui Qin[1,2], Tengfei Zhang[1,2], Feng Li[1], Xinfeng Chen[1,2], Yu Ping[1,3], Dan Wang[1,2], Qun Gao[1,2], Qianyi He[1], Lan Huang[1], Hong Li[1], Jianmin Huang[1], Xuan Zhao[1], Wenhua Xue[4], Zhi Sun[4], Jingli Lu[4], Jane J. Yu[5], Jie Zhao[4], Bin Zhang[6], and Yi Zhang[1,2,3,7]

Abstract

Metformin is a broadly prescribed drug for type 2 diabetes that exerts antitumor activity, yet the mechanisms underlying this activity remain unclear. We show here that metformin treatment blocks the suppressive function of myeloid-derived suppressor cells (MDSC) in patients with ovarian cancer by downregulating the expression and ectoenzymatic activity of CD39 and CD73 on monocytic and polymononuclear MDSC subsets. Metformin triggered activation of AMP-activated protein kinase α and subsequently suppressed hypoxia-inducible factor α, which was critical for induction of CD39/CD73 expression in MDSC. Furthermore, metformin treatment correlated with longer overall survival in diabetic patients with ovarian cancer, which was accompanied by a metformin-induced reduction in the frequency of circulating $CD39^+CD73^+$ MDSC and a concomitant increase in the antitumor activities of circulating $CD8^+$ T cells. Our results highlight a direct effect of metformin on MDSC and suggest that metformin may yield clinical benefit through improvement of antitumor T-cell immunity by dampening CD39/CD73-dependent MDSC immunosuppression in ovarian cancer patients.

Significance: The antitumor activity of an antidiabetes drug is attributable to reduced immunosuppressive activity of myeloid-derived tumor suppressor cells. *Cancer Res; 78(7); 1779–91. ©2018 AACR.*

Introduction

Immunosuppression is mediated by factors released from the tumor or by infiltration of different immunosuppressive cells in the tumor-suppressive microenvironment such as myeloid-derived suppressor cells (MDSC; refs. 1–4) and regulatory T cells (5). MDSCs expand in tumor-bearing individuals and suppress T-cell responses via various mechanisms. Increased number of MDSCs has been observed in the blood, lymph nodes, bone marrow (BM), and tumor sites of patients with cancer, acute and chronic inflammation, traumatic stress, and transplantation (1, 6). In a variety of human tumor types, MDSCs are mainly defined as two subpopulations of cells, including monocytic (M-MDSC) and polymononuclear MDSC (PMN-MDSC; refs. 7–9). Accumulation of functional MDSCs has been demonstrated to be a main contributor to tumor-induced immunosuppression (10–12). Thus, a number of therapeutic approaches to overcome MDSC-induced immunosuppression are under clinical development (13–15). However, the molecular mechanisms that regulate MDSCs in human cancer immunopathogenesis still remain obscure.

Ectonucleotidases are localized on the tumor cells and different populations of immune cells that hydrolyze ATP or ADP into AMP by the CD39 (ectonucleoside triphosphate diphosphohydrolase-1) and further processed into adenosine by the CD73 (ecto-5′-nucleotidase) in the tumor microenvironment (16–18). We and others have demonstrated the pivotal role of CD39/CD73-mediated adenosinergic pathways in tumor growth and metastasis through regulation of antitumor T-cell immunity (19–21). More recently, we show that CD39/CD73-mediated ectoenzymatic activity contributes significantly to immunosuppression by both mouse (22) and human MDSCs (23).

Metformin (dimethylbiguanide), a prescribed drug for type 2 diabetes, has been reported to have anticancer effects and reduce the frequency and mortality of specific cancers, particularly in

[1]Biotherapy Center, The First Affiliated Hospital of Zhengzhou University, Zhengzhou, Henan, P.R. China. [2]Cancer Center, The First Affiliated Hospital of Zhengzhou University, Zhengzhou, Henan, P.R. China. [3]School of Life Sciences, Zhengzhou University, Zhengzhou, Henan, P.R. China. [4]Department of Pharmacy, The First Affiliated Hospital of Zhengzhou University, Zhengzhou, Henan, P.R. China. [5]Department of Internal Medicine, Pulmonary, Critical Care and Sleep Medicine, University of Cincinnati College of Medicine, Cincinnati, Ohio. [6]Division of Hematology/Oncology, Department of Medicine, Robert H. Lurie Comprehensive Cancer Center, Northwestern University Feinberg School of Medicine, Chicago, Illinois. [7]Key Laboratory for Tumor Immunology and Biotherapy of Henan Province, Zhengzhou, Henan, China.

Note: Supplementary data for this article are available at Cancer Research Online (http://cancerres.aacrjournals.org/).

L. Li, L. Wang, and J. Li contributed equally to this article.

Corresponding Authors: Yi Zhang, The First Affiliated Hospital of Zhengzhou University, No. 1 Jianshe East Road, Zhengzhou 450052, Henan, China. Phone: 15138928971; Fax: 86-371-66970906; E-mail: yizhang@zzu.edu.cn; and Bin Zhang, Division of Hematology/Oncology, Department of Medicine, Robert H. Lurie Comprehensive Cancer Center, Northwestern University Feinberg School of Medicine, Chicago, IL 60611. E-mail: bin.zhang@northwestern.edu

doi: 10.1158/0008-5472.CAN-17-2460

long-term users (24, 25). Metformin has been shown capable of facilitating cell-cycle arrest and inducing apoptosis. It also appears to preferentially kill cancer-initiating/stem cells via AMP-activated protein kinase (AMPK) activation (26–28). Despite the chemopreventive activity, little is known about the effect of metformin on antitumor immune responses.

Apart from the inhibitory effect of metformin on cancer cells, we here demonstrate the direct action of metformin on MDSCs, which is linked to improvement of antitumor $CD8^+$ T-cell functionality and increased overall survival of patients with ovarian cancer. Importantly, MDSC-mediated immunosuppression is diminished by metformin treatment, depending on inhibition of CD73/CD39 expression on MDSCs through activation of AMPKα and inhibition of the hypoxia-inducible factor α (HIF1α) pathway. Our study thus reveals a novel antitumor mechanism of metformin administration that may restore antitumor T-cell immunity by impairing the suppressive function of MDSCs to yield clinical benefit.

Patients and Methods

Donor recruitment and sample preparation

From November 2013 to November 2015, 52 patients with ovarian cancer from the First Affiliated Hospital of Zhengzhou University were enrolled. The patients had not been treated with anticancer drugs, radiotherapy, or surgery in the beginning of the study and had no other systemic diseases. Clinical stages were classified according to the International Union against Cancer. Peripheral blood mononuclear cells (PBMC) were obtained from 52 patients with ovarian cancer and 25 healthy donors with similar gender and age distribution, respectively. Tumor tissues were obtained from 31 patients with ovarian cancer for the isolation of tumor-infiltrating leukocytes (TIL). The overall survival analysis with adjustments for confounders, including age, histologic subtype, grade, body mass index, smoking, type of surgery, postoperative residual disease, and chemotherapy drug delivery approaches, was obtained from those ovarian cancer patients with diabetes who received metformin ($n = 50$) and did not ($n = 34$) in electronic medical records from January 2013 to December 2016 in the First Affiliated Hospital of Zhengzhou University. The peripheral blood of 18 patients with primary diabetes was measured before and after metformin treatment in the department of endocrinology. Fresh human PBMCs and TILs were harvested as previously described (4). All patients gave written informed consent. The whole consent procedure was in accordance with the Declaration of Helsinki and the standard defined by Institutional Review Boards of the First Affiliated Hospital of Zhengzhou University.

Antibodies and flow cytometry

The number of 1×10^5 cells were harvested from fresh human PBMCs and TILs that were stained with anti-CD3 (PerCP-Cy 5.5 or APC-conjugated from BD Biosciences), anti-CD8 (PerCP-conjugated from BD Biosciences), anti-7AAD (PerCP-conjugated from BD Biosciences), anti-CD14 (APC-Cy7 or Percp-conjugated from BD Biosciences), and anti-CD11b (PE-cy7-conjugated from BD Biosciences). The following fluorescence-conjugated antibodies were also used:CD15 (Percp), CD33 (FITC and PE), HLA-DR (APC and PE), CD39 (APC), CD73 (FITC), CD124 (PE), CD56 (PE), CD19 (FITC), Ki-67 (PE), Annexin V (APC), granzyme B (PE), IFNγ (APC), and perforin (FITC) obtained from BD Biosciences (Supplementary Table S1). Among them, granzyme B, IFNγ, and perforin were stained intracellularly as follows: cells were first fixed with 2% paraformaldehyde and permeabilized with 0.1% saponine–PBS buffer. Next, cells were incubated for 15 minutes on ice with antibodies labeled with fluorochrome in the darkness. For surface assessment, cells were incubated with fluorochrome-labeled antibodies directly. In each case, isotypic control was performed. PBMCs were stained according to the manufacturer's instructions. The appropriate isotype-matched control antibodies were purchased from BD Biosciences. Cells were analyzed using a FACS Canto II flow cytometer (BD) and Diva analysis software (BD).

Cell isolation and sorting

Ovarian biopsy specimens ($n = 31$) were cut into small pieces and digested in RPMI 1640 (Gibco) supplemented with 0.25% trypsin (Gibco), 0.002% DNaseI (Gibco), and 20% FBS (Gibco) at 37°C for 20 minutes. TILs within dissociated cells were filtered through a 100 μm mesh and isolated by Ficoll–Hypaque density gradient centrifugation (Beijing Chemical Reagent Company). The mononuclear cells were washed and resuspended in medium supplemented with 10% heat-inactivated FBS for FACS analysis. PBMCs were isolated by Ficoll–Hypaque density gradient centrifugation, sequentially using the anti-CD14 and anti-CD11b MACS magnetic sorting system (Miltenyi Biotec) within 2 hours of sample collection. PMN-MDSCs ($CD14^-CD11b^+$) and M-MDSCs ($CD14^+CD11b^+$) were enriched according to the manufacturer's instructions. The purity of the two subsets of cells was >95%. $CD8^+$ T cells were further purified by MACS magnetic sorting system according to the manufacturer's protocol (Miltenyi Biotec), and the purity was also >95%. Then, $CD8^+$ T lymphocytes were magnetically isolated, as confirmed by flow cytometry.

Quantitative RT-PCR

Total RNA from PMN-MDSCs and M-MDSCs was extracted using the TRIzol Reagent (Invitrogen Life Technologies), and RNA using the total of 5 μg cDNA was synthesized from single-strand PrimeScript RT Reagent Kit with gDNA eraser (TaKaRa). The concentration and purity of all total RNA samples were verified using NanoDrop2000 (Thermo Scientific). The cDNA was obtained using a PrimeScript RT Reagent Kit (TaKaRa) according to the instruction. Briefly, samples containing 1 μg total RNA were incubated with 1 μL gDNA Eraser, 2 μL 5x cDNA Eraser Buffer, and RNase free dH_2O at 42°C for 2 minutes. After adding the enzyme mix to the annealed total RNA sample, the reaction was incubated for 15 minutes at 37°C. Quantitative real-time was done using SYBR Premix Ex Taq II (Takara, RR820A) and was assessed by outcarried PCRs (Agilent Mx3005P). Samples were amplified using the following conditions: 40 cycles of 95°C/30 seconds, 95°C/5 seconds, 60°C/30 seconds. Relative gene expression was determined by normalizing the expression of each target gene to GAPDH. The data were analyzed by $2^{-\Delta\Delta C_t}$. Primer sequences for all gene-specific amplifications were shown in Supplementary Table S2.

$CD8^+$ T-cell suppression assay

PMN-MDSCs ($Lin^-CD14^-CD11b^+CD15^+HLA\text{-}DR^{low/neg}$) and M-MDSCs ($Lin^-CD14^+CD11b^+CD15^-HLA\text{-}DR^{low/neg}$) purified from peripheral blood of ovarian cancer patients or healthy donors as targets were incubated in a 24-well U bottom plate, and at effector: targeted (E:T) ratios of 0:1, 1:1, and 4: 1 with

autologous $CD8^+$ T cells (10^5 per well) as effector cells stimulated by 30 ng/mL anti-CD3/anti-CD28 (Miltenyi Biotech). 2-Methoxyestradiol (2-MeOE2), an HIF1α inhibitor, and 120 μmol/L cobalt (II) chloride ($CoCl_2$,Sigma-Aldrich) were added to the 24-well U bottom plate at the 0:1, 1:1, and 4:1 E: T ratios, and incubated for 24 hours. To examine the importance of CD39/CD73 activity, MDSCs were pretreated with ARL67165, a CD39 inhibitor (250 μmol/L; Sigma-Aldrich), and/or APCP, a CD73 inhibitor (100 μmol/L; Sigma-Aldrich), for 30 minutes before adding the $CD8^+$ T cells. To measure the function of $CD8^+$ T cells suppressed by MDSCs, $CD8^+$ T cells were stimulated with 1 mg/mL phorbolmyfismteacetate (PMA, Sigma-Aldrich), 50 ng/mL ionomycin (Sigma-Aldrich), and 5 mg/mL brefeldin A solution (BFA, Biolegend) for 4 hours at 37°C in 5% CO_2 atmosphere prior to harvesting, and then intracellular IFNγ, granzyme B, and perforin production (Biolegend) were determined by flow cytometry.

Animal experiment

Animal protocols were approved by the Review Board of the First Affiliated Hospital of Zhengzhou University. Female BALB/c-nu mice (15–18 g, 4–6-week old) were obtained from the animal facility (Beijing Vital River Laboratory Animal Technology Co., Ltd.) and randomly segregated into 2 groups with 3 mice in each group. The First Affiliated Hospital of Zhengzhou University provides human primary ovarian solid tumor tissues. Tumor tissue was mechanically disrupted using a scissors to generate clusters or aggregates of cells that passed through a size 50 stainless steel wire mesh. The resulting tumor-derived cell aggregates were washed once in RPMI 1640 and resuspended in PBS. Suspensions of tumor-derived cell aggregates were injected subcutaneously into the left flank of recipient BALB/c-nu mice. Each mouse received between 100 and 300 mg of the cell aggregates in a volume of 1.0 mL until about 2 weeks. The treatment group of BALB/c-nu mice received 10 mmol/L metformin (Sigma-Aldrich) in PBS by oral gavage every day till day 35. The control mice received vehicle alone. To analyze the effects of metformin treatment, TILs were collected from the tumor tissue of experimental and control mice. The tissue from each mouse was grinded and diluted 10-fold with the RBC lysis buffer. The cells were washed with PBS followed by a second wash in FACS buffer [2% heat-inactivated FBS and 2 mmol/L ethylenediaminetetraacetic acid (EDTA)] in PBS. The cells collected from each mouse were resuspended in equal volume of FACS buffer. Fluorophore-conjugated human-specific antibodies CD3-Percp, CD14-APC-Cy7, CD11b-PE-Cy7, CD39-APC, and CD73-FITC were purchased from Invitrogen (Biolegend). The samples to be analyzed were first incubated with human FcR blocking reagent at 4°C in dark for 15 minutes (#130-059-90; Miltenyi Biotech). The cells were then washed and appropriate antibodies were added to each set of cells, and the samples were incubated on ice for 30 minutes in dark. The samples were then washed and resuspended in 300 μL of FACS buffer. The cell phenotype was determined using cytofluorimetric analysis by flow cytometer (BD Biosciences).

Western blot analysis

PMN-/M-MDSCs were extracted into cold lysis buffer containing 50 mmol/L Tris-HCl (pH 7.5), 150 mmol/L NaCl, 1 mmol/L EDTA, 1 mmol/L $MgCl_2$, 0.5% Triton X-100, phosphatase inhibitor mix (1 mmol/L NaF, 1 mmol/L Na_3VO_4, and 1 mmol/L β-glycerol phosphate), and protease inhibitor mix [1 mmol/L PMSF, 2 μg/mL Roche (cocktail: inhibitor protease aprotinin), 1 μg/mL leupeptin, and 1 μg/mL pepstatin A]. Complete cell lysates were clarified by centrifugation at 12,000 × *g* content for 15 minutes, subjected to SDS-PAGE (8%–10% polyacrylamide gels), and then transferred onto PVDF membranes (Millipore). The membrane was blocked in TBS-T buffer (20 mmol/L Tris-Hcl, pH 7.5, 150 mmol/L NaCl, and 0.05% Tween-20) containing 5% (w/v) nonfat milk at room temperature (22°C) for 1 hours and then probed with antibodies for total and phosphorylated AMPKα (Cell Signaling Technology), total HIF1α (Cell Signaling Technology; D2U3T), and GAPDH (Santa Cruz Biotechnology) at 4°C overnight, followed by incubation with horseradish peroxidase–conjugated anti-IgG for 1 hour at room temperature. Detection was performed with the SuperSignal West Femto Maximum Sensitivity Substrate Trial Kit (Pierce). The band images were digitally captured and quantified with a Fluor Chem FC2 imaging system (Alpha Innotech).

Reactive oxygen species detection

Intracellular reactive oxygen species (ROS) was determined using a fluorescent probe DCFH-DA. Cells were pretreated with 4 μmol/L carboxy-2′, 7′-dichlorodihydrofluorescein diacetate (H2DCFDA; Sigma) and then stained with surface markers to monitor the ROS level in cells.

Measurement of CD39/CD73 activity by HPLC-MS analysis

To determine the effect of metformin on enzyme activity of CD39 and CD73 in MDSCs, we measured the conversion of extracellular AMP to adenosine (ADO; CD73 activity) and extracellular ATP and ADP to AMP (CD39 activity) by HPLC-MS analysis as described previously (29). In brief, purified PMN-MDSCs and M-MDSCs in the absence or presence of metformin (final concentration 2 mmol/L) were incubated at 37°C for 12 hours with exogenous 100 μmol/L ATP (Sigma-Aldrich) and ARL67165 (CD39 inhibitor, 250 μmol/L) or 100 μmol/L AMP (Sigma-Aldrich) and APCP (CD73 inhibitor, 100 μmol/L). Supernatants from the cell cultures were harvested by centrifugation at 200 × *g* for 6 minutes at 4°C to remove the cells. Supernatants were filtered (0.22 μm) and frozen (−20°C) until analysis via LC-MS. The chromatography was operated on an ACQUITY UPLC system (Waters Corp.) with cooling autosampler and column oven. The separation was conducted on an ACQUITY UPLC BEH C_{18} column (2.1 mm × 50 mm, 1.7 μm) at 40°C. The mobile phase consisted of acetonitrile (A) and 0.1% formic acid water (B). The elution program was as follows: 0–5 minutes, 10% A. The flow rate was 0.2 mL/min. Mass spectrometric detection was carried out on a Xevo TQD triple-quadrupole tandem mass spectrometer (Waters Corp.) equipped with an electrospray ionization interface. Quantitative analysis was performed in selected ion monitoring (SIR) mode, and the quasimolecular ions were m/z ADO (267.70), m/z AMP (347.50), m/z ADP (427.90), and m/z ATP (507.70). CD39/CD73 activity was expressed as percent AMP conversion in this time frame.

Statistical analysis

Based on the distribution level, data were reported as mean ± SD, and correlation analyses were evaluated with parametric (independent-sample or paired *t* test and Spearman test) or nonparametric (Wilcoxon and Spearman ρ test) tests. Significant

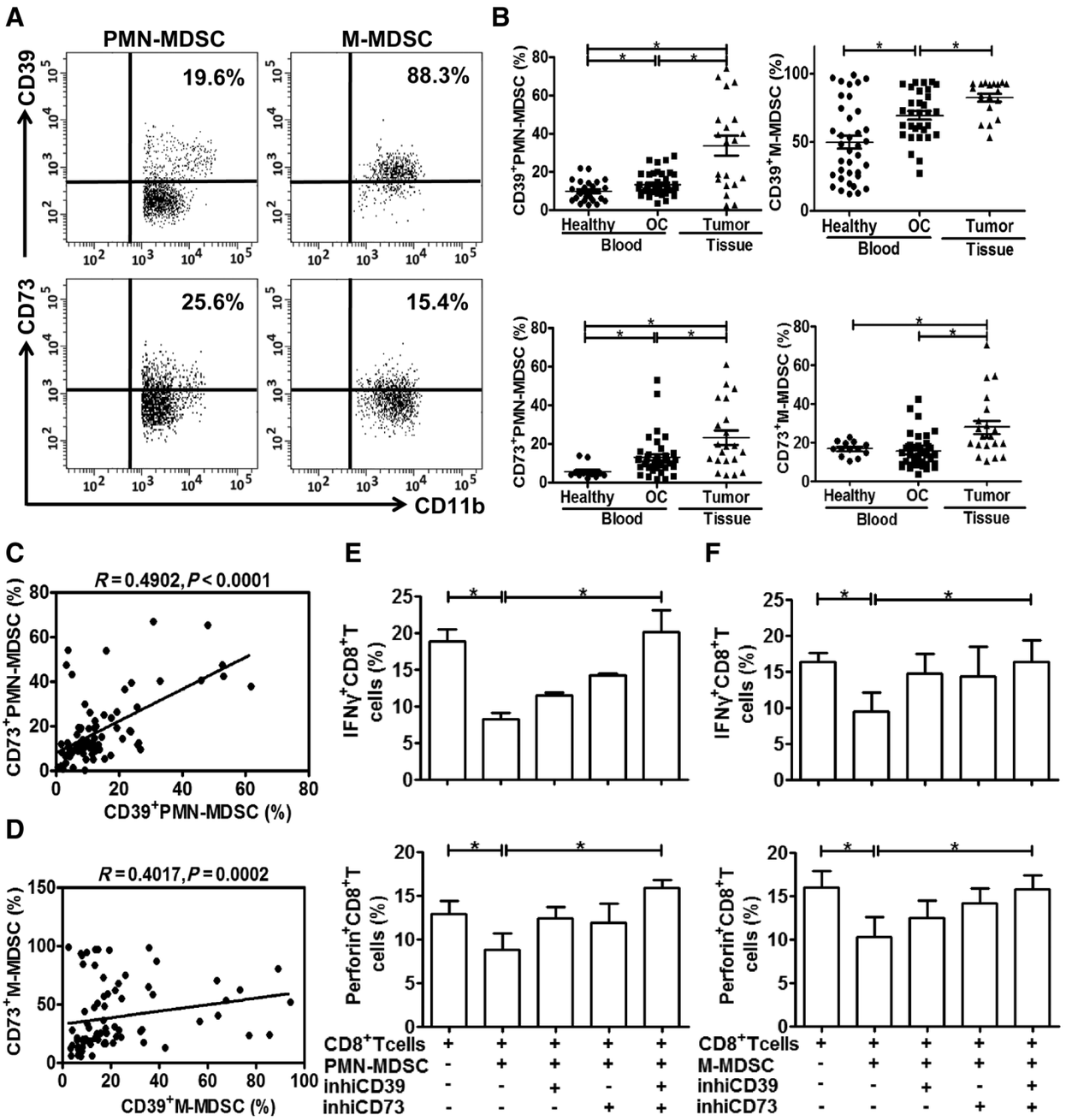

Figure 1.

CD39/CD73 expressed on MDSCs in ovarian cancer (OC) patients mediates MDSC's suppressive activity. **A,** The representative flow cytometry analysis of CD39 and CD73 expression on PMN-MDSCs ($CD3^-CD19^-CD56^-CD11b^+CD14^-HLA\text{-}DR^{low/neg}$) and M-MDSCs ($CD3^-CD19^-CD56^-CD11b^+CD14^+HLA\text{-}DR^{low/neg}$) from patients with ovarian cancer. **B,** The percentages of CD39 and CD73 expression on PMN-MDSCs and M-MDSCs from peripheral blood ($n = 42$) and matched tumor tissues ($n = 26$) of patients with ovarian cancer. The peripheral blood of healthy donors ($n = 16$) was measured as control. The correlation between the expression levels of CD39 and CD73 on PMN-MDSCs (**C**) or M-MDSCs (**D**) was established by Spearman ρ analysis. *, $P < 0.05$. Sorted PMN-MDSCs (**E**) or M-MDSCs (**F**) from ovarian cancer patients were cultured with autologous $CD8^+$ T cells at a ratio of 1:4 in the absence or presence of CD39 inhibitors (ARL67156) and/or CD73 inhibitors (APCP) for 3 days ($n = 4$). Production of IFNγ or perforin in $CD8^+$T cells was measured by flow cytometry. Data are given as mean ± SD. *, $P < 0.05$.

differences ($P < 0.05$) were determined using one-way ANOVA, two-tailed t test, or one-tailed t test, as indicated in figure legends. Outliers were detected by a Grubb test. Significant correlations were determined using two-tailed (or one-tailed where designated) Pearson correlation calculations. All statistics and graph preparations were performed using Prism 6 (Graph Pad Software Inc.).

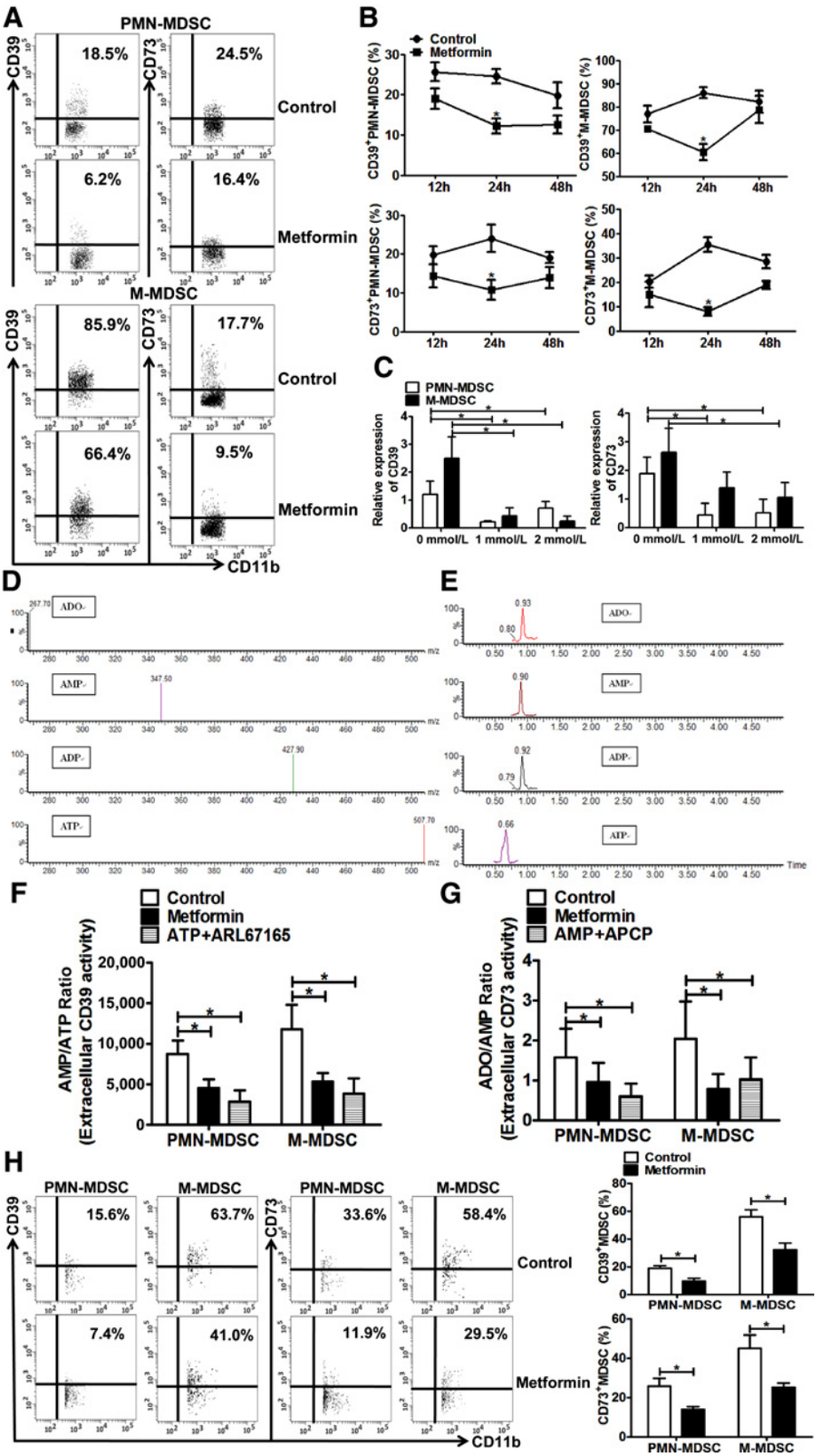

Figure 2.

Metformin reduces the expression and enzymatic activity of CD39 and CD73 on MDSCs. **A,** The representative flow cytometry analysis of CD39/CD73 expression on purified ovarian cancer PMN-MDSCs and M-MDSCs treated with 2 mmol/L metformin or control solvents for 48 hours ($n = 3$). **B,** The expression levels of CD39 and CD73 on PMN-MDSCs or M-MDSCs were determined at indicated times by flow cytometry. **C,** The gene expression of CD39 and CD73 in purified PMN-MDSCs and M-MDSCs 24 hours after treatment of metformin or control solvents was measured by qRT-PCR. Relative gene expression was determined by normalizing the expression of each target gene to GAPDH. Purified PMN-MDSCs and M-MDSCs were treated with 2 mmol/L metformin in the presence of exogenous ATP and ARL67165 (CD39 inhibitor) or AMP and APCP (CD73 inhibitor) or control solvents for 12 hours. Representative HPLC-MS graphs show the peak resolution (**D**) and retention time (**E**) of metabolites of adenylate, including ATP, ADP, AMP, and ADO. The CD39 and CD73 enzymatic activity was determined by HPLC-MS analysis of extracellular ATP conversion to ADP (**F**) and extracellular AMP conversion to ADO (**G**), respectively. **H,** Flow cytometry analysis of CD39/CD73 expression on human ovarian tumor-infiltrating PMN-MDSC and M-MDSC in nude mice ($n = 3$) treated by 10 mmol/L metformin or control vehicles. Data are representative of three independent experiments. Data are given as mean ± SD. *, $P < 0.05$.

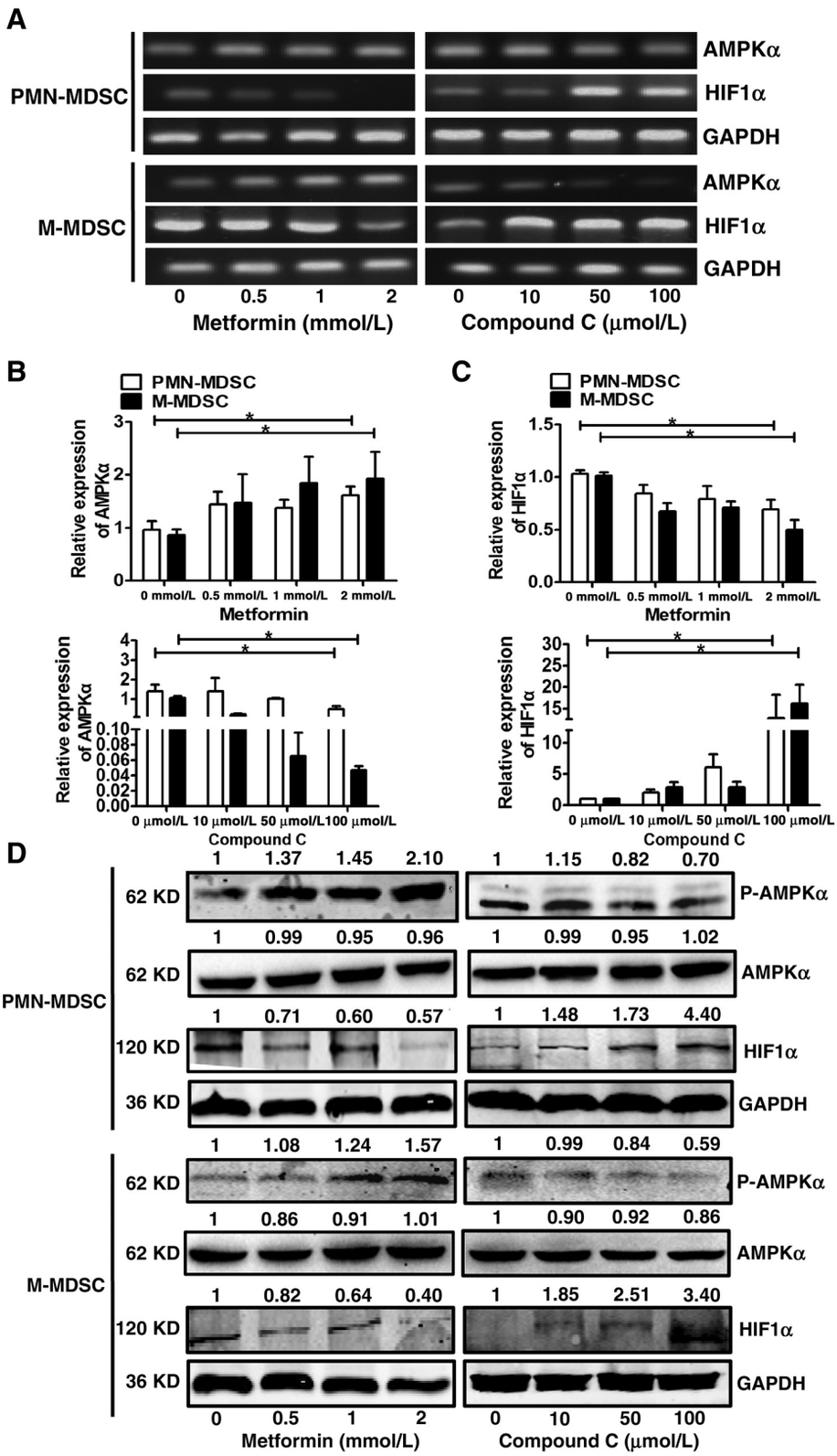

Figure 3.

Metformin inhibits HIF1α via activation of AMPKα in MDSCs. **A–C,** The gene expression of AMPKα and HIF1α in purified PMN-MDSCs and M-MDSCs from peripheral blood of ovarian cancer patients was measured 24 hours after treatment of metformin or Compound C (AMPK inhibitors) at indicated doses using qRT-PCR. Relative gene expression was determined by normalizing the expression of each target gene to GAPDH. **D,** The protein expression of total and phosphorylated AMPKα and total HIF1α in purified PMN-MDSCs and M-MDSCs from peripheral blood of ovarian cancer patients 24 hours after treatment with metformin or Compound C at indicated doses was measured by Western blot. Anti-GAPDH was used as a loading control. Data are representative of three independent experiments. Data are given as mean ± SD. *, $P < 0.05$.

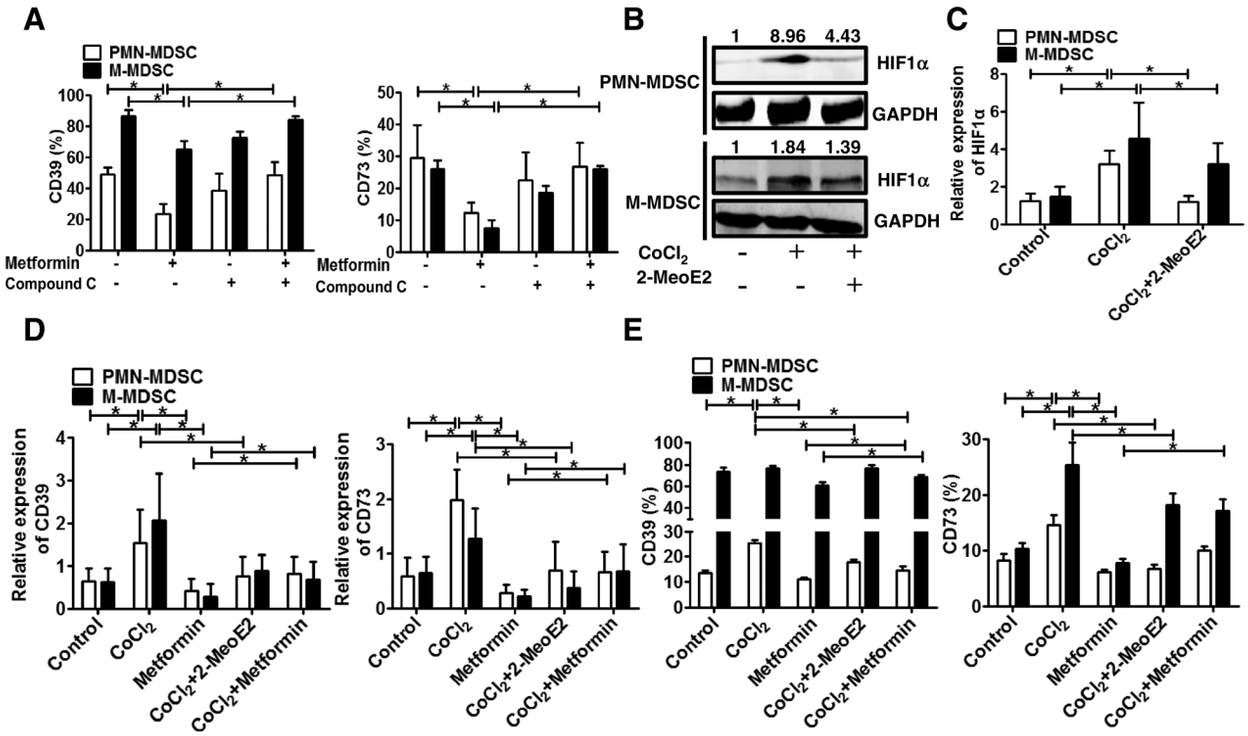

Figure 4.

Metformin reduces the expression of CD39 and CD73 to limit the suppressive activity of MDSCs via the AMPKα/HIF1α pathway. **A,** Flow cytometry analysis of CD39 and CD73 expression on purified PMN-MDSCs and M-MDSCs from peripheral blood of patients with ovarian cancer in the absence or presence of 2 mmol/L metformin and/or 100 μmol/L Compound C for 24 hours. Expression levels of HIF1α in purified PMN-MDSCs and M-MDSCs were measured by Western blot (**B**) and qRT-PCR (**C**) 24 hours after treatment with $CoCl_2$ and/or 2-MeoE2 (HIF1α inhibitor) *in vitro*. Expression of CD39 and CD73 on purified PMN-MDSCs and M-MDSCs treated with reagents as indicated for 24 hours was analyzed by qRT-PCR (**D**) and flow cytometry (**E**). Data ($n = 5$) are given as mean ± SD. *, $P < 0.05$.

Results

Elevated expression of functional CD39/CD73 on MDSCs in patients with ovarian cancer

The percentages of $CD14^-CD11b^+$ and $CD14^+CD11b^+$ cells were determined in Lin^- ($CD3^-CD56^-CD19^-$) mononuclear cells. The PMN-MDSCs were indicated as $Lin^-CD14^-CD11b^+CD15^+HLA\text{-}DR^{low/negative}$ and M-MDSCs as $Lin^-CD14^+CD11b^+CD15^-HLA\text{-}DR^{low/negative}$ (Supplementary Fig. S1A) as described previously (30). In line with the previous studies (4, 31), the frequencies of PMN-MDSCs (Supplementary Fig. S1B) and M-MDSCs (Supplementary Fig. S1C) were both higher in peripheral blood and tumor tissues of patients with ovarian cancer than those in normal donors. Interestingly, the frequency of PMN-MDSCs was higher than that of M-MDSCs in ovarian cancer patients, but lower in healthy donors (Supplementary Fig. S1D). As expected, MDSCs from ovarian cancer patients expressed higher level of typical MDSC-associated suppressive markers including TNFα, COX-2, IL10, arginase1 (ARG1), and TGFβ than those from healthy donors (Supplementary Fig. S2A). We also confirmed that both subsets of MDSCs mediated their inhibitory effect on $CD8^+$ T-cell proliferation and functions (Supplementary Fig. S2B).

We and others have reported that MDSCs suppress T-cell immunity through the enzymatic activity of CD39/CD73 in mouse models (22, 32). To determine the role of CD39/CD73 on MDSC in human tumor immunopathology, we showed that the proportion of $CD39^+$ and $CD73^+$ MDSCs in peripheral blood from ovarian cancer patients was significantly higher than that from healthy donors (Fig. 1A and B). There were the markedly elevated levels of CD39/CD73 expression on both MDSC subsets in tumor tissues compared with peripheral blood from patients or healthy donors. Furthermore, expression levels of CD39 on both MDSC subsets were positively correlated with the levels of CD73 (Fig. 1C and D). We purified both MDSC subsets from ovarian cancer patients and cocultured with autologous $CD8^+$ T cells in the presence or absence of CD39/CD73 enzymatic inhibitors (ARL67156 and/or APCP). As expected, the production of IFNγ or perforin from $CD8^+$ T cells was inhibited by both MDSC subsets. However, this effect was diminished by blockade of CD39 and CD73 activities using their inhibitors (Fig. 1E and F). These findings indicate that CD39 and CD73 ectonucleotidase activities may contribute to MDSC-mediated immunosuppression *in vitro*.

Metformin reduces the expression and activity of CD39 and CD73 on MDSCs

Both MDSC subsets were purified from ovarian cancer patients and subject to metformin effect on CD39/CD73 expression by MDSCs. We found reduced expression levels of CD39/CD73 on both MDSC subsets 24 hours after metformin treatment *in vitro* by flow cytometry (Fig. 2A and B). Likewise, metformin treatment

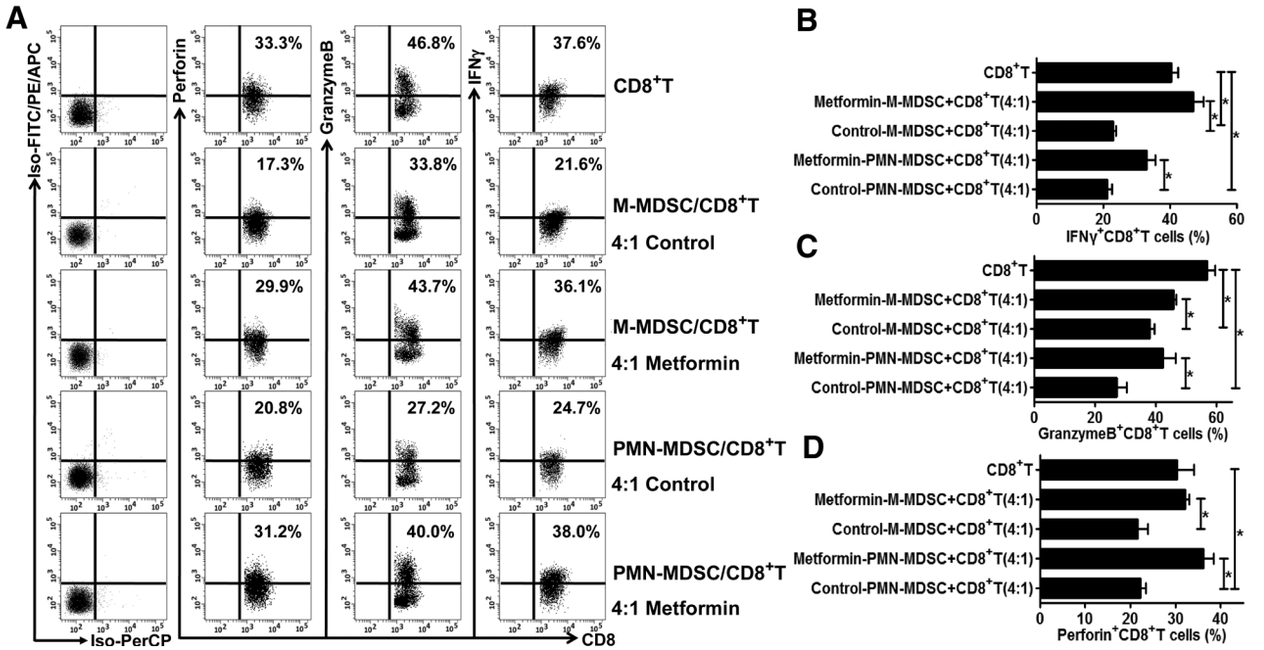

Figure 5.

Metformin diminishes MDSC-mediated immunosuppression *in vitro*. PMN-MDSCs or M-MDSCs sorted from ovarian cancer patients were cultured with autologous $CD8^+$ T cells at a ratio of 1:4 in the presence of 2 mmol/L metformin or control solvents for 24 hours ($n = 5$). **A-D,** The representative flow cytometry dot plots showing $CD8^+$ T-cell secretory function (**A**), and the summary graph showing production of IFNγ (**B**), granzyme B (**C**), or perforin (**D**) in $CD8^+$ T cells was measured by flow cytometry. Data (mean ± SD) are representative of three independent experiments. *, $P < 0.05$.

decreased mRNA expression of CD39/CD73 on both MDSC subsets by qRT-PCR (Fig. 2C). However, there were no significant differences in expression levels of a number of inhibitory molecules including COX-2, TNFα, IL10, TGFβ, iNOS, and ARG1 and ROS production in MDSCs between the metformin treatment and control groups (Supplementary Fig. S3A and S3B). We further asked whether metformin can affect the ectoenzymatic activity of CD39/CD73 on MDSCs. CD39, an ecto-apyrase that converts ATP/ADP to AMP and extracellular AMP, is metabolized to adenosine (ADO) by MDSC-expressed CD73 (29). The typical production mass spectra and selected reaction monitoring chromatograms of ATP, ADP, AMP, and ADO were detected by HPLC-MS using quantitative analysis in selected ion monitoring (SIR) mode (Fig. 2D and E). As expected, metformin decreased the production of AMP from extracellular ATP and ADO from extracellular AMP in supernatants of MDSC cultures, indicating that metformin inhibited the enzymatic activity of CD39 in the conversion of ATP to AMP and CD73 activity in the conversion of AMP to ADO (Fig. 2F and G). To examine the *in vivo* effect of metformin on MDSCs, we grew the human ovarian cancer tissues on nude mice after subcutaneous inoculation. Consistent with the *in vitro* results above, we found decreased expression of CD39 and CD73 on tumor-infiltrating MDSCs 35 days after metformin treatment (Fig. 2H).

Metformin modulates the expression of CD39 and CD73 on MDSCs via AMPKα and HIF1α pathway

To search the molecular mechanism of metformin-mediated regulation of CD39 and CD73 expression on MDSCs, we first measured the expression levels of AMPKα and HIF1α in purified PMN-MDSCs and M-MDSCs treated with metformin (AMPK activator) or Compound C (AMPK inhibitor) by qRT-PCR (Fig. 3A–C) and Western blot (Fig. 3D). As expected, metformin augmented AMPKα phosphorylation while reduced HIF1α expression in both MDSC subsets in a dose-dependent manner. In contrast, treatment of Compound C reduced AMPKα phosphorylation while augmented HIF1α expression in both MDSC subsets in a dose-dependent manner. The data suggest that HIF1α is likely a downstream target of AMPKα triggered by metformin.

Given the pivotal role of HIF1α for induction of CD73/CD39 expression, we thus tested if metformin modulated CD73/CD39 expression on MDSCs via AMPKα and HIF1α pathways. Metformin treatment decreased the expression of CD39 and CD73 on both MDSC subsets, but the effect was abrogated by addition of Compound C (Fig. 4A). To examine the role of HIF1α in this process, we confirmed the increased HIF1αexpression 24 hours after $CoCl_2$-induced hypoxia but attenuated HIF1α expression by addition of HIF1α inhibitor 2-MeOE2 in purified MDSCs using Western blot (Fig. 4B) and qRT-PCR (Fig. 4C). In line with these results, we showed that treating MDSCs with $CoCl_2$ increased the expression of CD39 and CD73 by qRT-PCR (Fig. 4D) and flow cytometry (Fig. 4E), whereas the effect was abrogated by addition of either 2-MeoE2 or metformin (Fig. 4D and E). Moreover, compared with metformin treatment alone, $CoCl_2$ rescued the inhibitory effect of metformin on CD39/CD73 in MDSCs (Fig. 4D and E). Taken together, these data suggest that metformin decreases the expression of CD39 and CD73 on MDSCs through activation of AMPKα and inhibition of the HIF1αpathway.

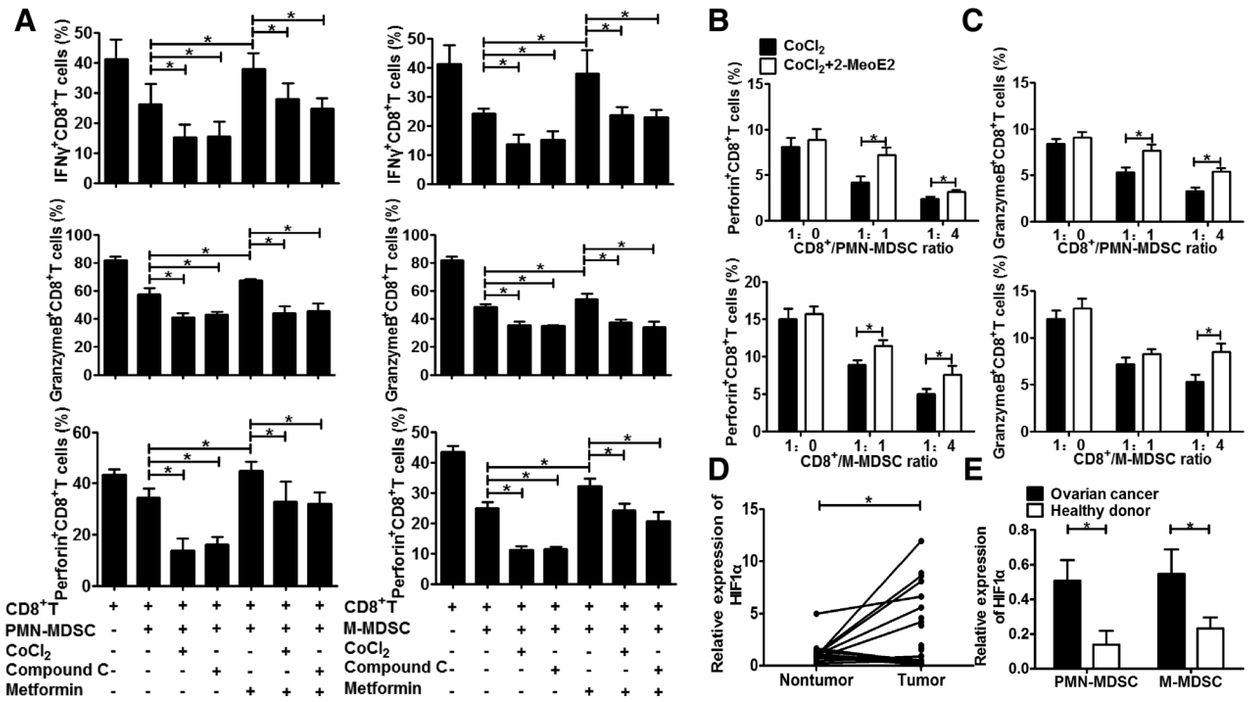

Figure 6.

MDSC-mediated immunosuppression depends on the AMPKα/HIF1α pathway. **A,** PMN-MDSCs or M-MDSCs sorted from ovarian cancer patients were cultured with autologous $CD8^+$T cells at a ratio of 1:4 in the absence or presence of 2 mmol/L metformin with or without 100 μmol/L Compound C and 120 μmol/L $CoCl_2$ for 24 hours, and the summary graph showing production of IFNγ, granzyme B, and perforin in $CD8^+$ T cells was measured by flow cytometry. The flow cytometry analysis of $CD8^+$ T cells producing granzyme B or perforin cultured with/without MDSCs at the indicated ratios for 24 hours. The percentage of granzyme B^+CD8^+ T cells (**B**) or $perforin^+CD8^+$ T cells (**C**) was summarized ($n = 5$). **D,** The relative expression of HIF1α from ovarian tumor tissues ($n = 26$) and ovarian cyst tissues ($n = 18$) was measured by qRT-PCR. **E,** The relative expression of HIF1α in purified PMN-MDSCs and M-MDSCs from peripheral blood of ovarian cancer patients ($n = 16$) versus healthy donors ($n = 13$) was analyzed by qRT-PCR. Data are given as mean ± SD. *, $P < 0.05$.

Metformin inhibits MDSC's suppressive activity by decreasing CD39 and CD73 expression on MDSCs

We have demonstrated that ectoenzymatic activity of CD39/CD73 on MDSCs contributes to MDSC's suppressive function (Fig. 1E and F; refs. 22, 23). Given the ability of metformin to inhibit CD39/CD73 expression and enzymatic activity of MDSCs, we tested if metformin could impair MDSC's suppressive activity by decreasing CD39/CD73 expression on MDSCs. Indeed, we found that metformin treatment diminished the suppressive effect of both MDSC subsets on production of IFNγ (Fig. 5A and B), granzyme B (Fig. 5A and C), or perforin (Fig. 5A and D) from $CD8^+$ T cells *in vitro*. As metformin modulated CD73/CD39 expression on MDSCs via AMPKα and HIF1α pathways (Fig. 5), we next examined the involvement of these pathways in the mechanism of MDSC-mediated suppressive activity toward T cells. Treatment of MDSCs with either $CoCl_2$ or Compound C alone potentiated the inhibitory effect of MDSCs on $CD8^+$ T-cell responses, whereas the effect was diminished by addition of metformin (Fig. 6A). Notably, compared with metformin treatment alone, addition of $CoCl_2$ or Compound C compromised the inhibitory action of metformin on MDSC-mediated suppressive activity (Fig. 6A), consistent with the results on their regulation onCD39/CD73 expression on MDSCs (Fig. 5). We further confirmed the role of HIF1α in MDSC-mediated suppressive activity. As shown in Fig. 6B and C, addition of HIF1α inhibitor 2-MeoE2 also significantly attenuated the suppressive effect of both MDSC subsets in the presence of $CoCl_2$ on production of granzyme B and perforin from $CD8^+$ T cells *in vitro* in a dose-dependent manner. In addition, we detected higher expression levels of HIF1α mRNA in ovarian tumor tissues than matched nontumor ovarian tissues by qRT-PCR (Fig. 6D). There was also elevated HIF1α expression in the purified two subsets of MDSCs from ovarian cancer patients compared with that in healthy donors (Fig. 6E)

To analyze the *in vivo* effect of metformin on MDSCs, expression levels of CD39/CD73 on MDSCs were compared by flow cytometry in ovarian cancer patients with diabetes between two groups before and after treatment of metformin. Consistent with the results described above, the percentages of $CD39^+$or $CD73^+$MDSCs were decreased in patients receiving metformin in this window of opportunity study, randomized trial (Fig. 7A and B). Further, we found increased production of granzyme B or perforin from $CD8^+$ T cells in these patients after metformin treatment compared with before treatment (Fig. 7C and D). Notably, overall survival of diabetic ovarian cancer patients receiving metformin treatment ($n = 50$) was longer than those not receiving metformin ($n = 34$, $P = 0.0068$; Fig. 7E; Supplementary Table S3). These results suggest a possibility that metformin may yield clinical benefit from improvement of antitumor T-cell immunity at least in part by

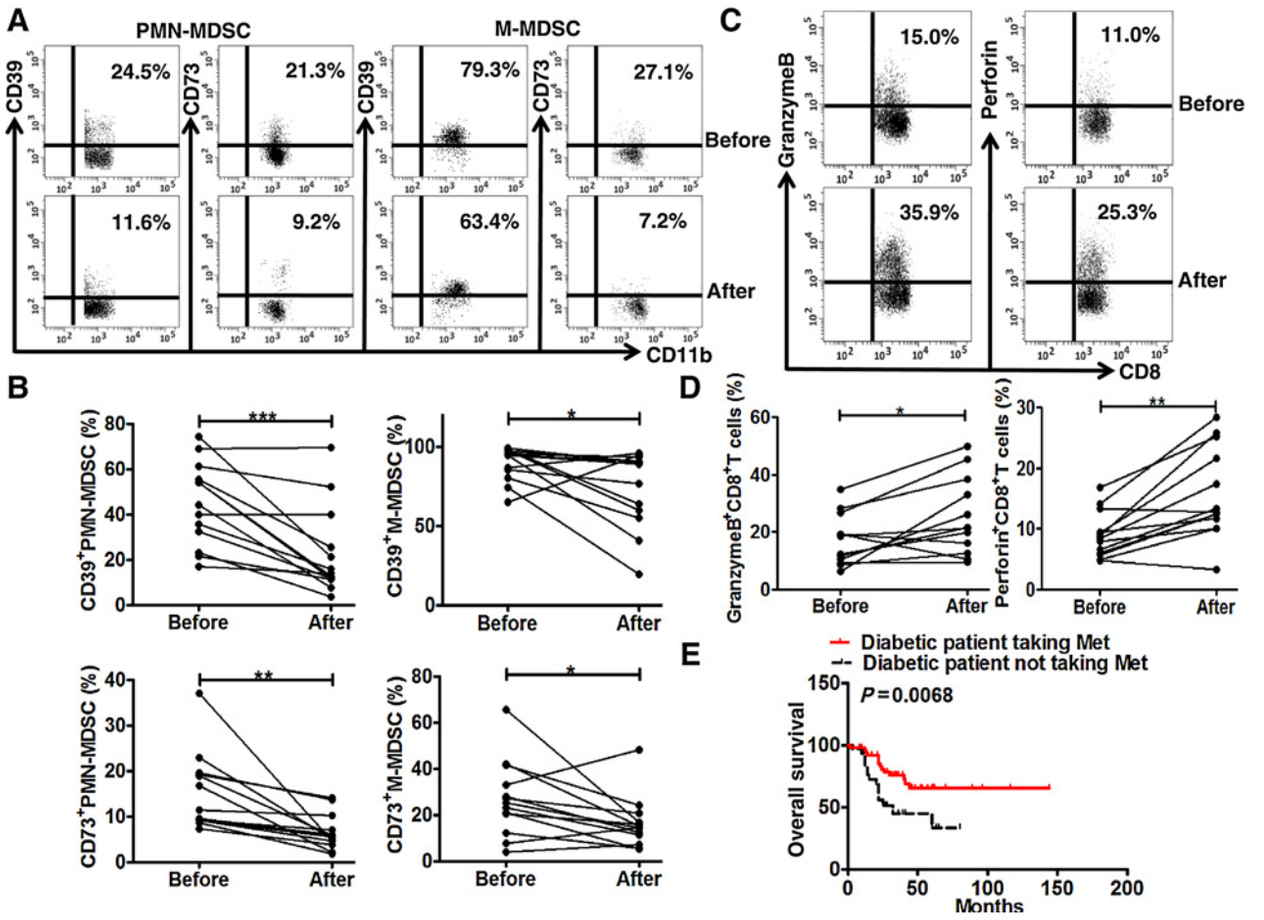

Figure 7.

Metformin treatment decreases expression of CD39 and CD73 on MDSCs and increases $CD8^+$ T-cell effector function in patients with diabetes. **A** and **B,** Expression of CD39 and CD73 on PMN-MDSCs or M-MDSCs from peripheral blood of patients with primary diabetes ($n = 18$) was measured before and after metformin treatment by flow cytometry. **C** and **D,** Production of perforin or granzyme B in $CD8^+$ T cells from peripheral blood of patients with primary diabetes ($n = 18$) was measured before and after metformin treatment by flow cytometry. Data are given as mean ± SD. *, $P < 0.05$; **, $P < 0.01$; ***, $P < 0.001$. **E,** Metformin intake was associated with the improved survival in ovarian cancer patients with diabetes. Overall survival was compared between ovarian cancer patients with diabetes who received metformin ($n = 50$) and those who did not ($n = 34$; $P = 0.0068$).

dampening CD39/CD73-dependent MDSC's suppressive activity in ovarian cancer patients.

Discussion

Although a recent study has reported a potential role of metformin for the differentiation and immunosuppressive function of mouse MDSCs *in vitro* (33), to the best of our knowledge, our study is the first to demonstrate that metformin may be involved in the regulation of human MDSC-mediated immunosuppression *in vitro* and *in vivo*. In this report, using human ovarian cancer as a model system, we explored the direct effect of metformin on MDSC's suppressive activity. Our results indicate that in addition to tumor-intrinsic effects, metformin also enhances $CD8^+$ T-cell activities by counteracting the immunosuppressive activity of MDSCs, which may facilitate tumor development and immune evasion.

Numerous preclinical and clinical studies have demonstrated direct antitumor activities for metformin. However, the precise causes and extent of metformin's antitumor effect remain elusive. Although metformin likely has pleiotropic effects on a wide array of cellular functions, its effect on immune system serves as an important proof-of-concept study. In particular, the role of metformin in tumor immunity is only beginning to be appreciated (34). There are several recent studies showing that metformin can promote $CD8^+$ memory T-cell generation (35, 36) and protect them from apoptosis and exhaustion in the tumor using experimental mouse tumor models (37). It is now becoming clear that metformin can directly act on T cells. Indeed, administration of metformin inhibited the Th1- and Th17 cell–mediated immune responses in mice (38, 39). Metformin was found further to attenuate Th1- and Th17-derived IL22 production and suppress tumor growth in an orthotopic mouse model of hepatocellular carcinoma (40). It will therefore be interesting to test whether metformin could exert dual effects on T cells and MDSCs to promote antitumor T-cell immune responses. Moreover, the possibility that metformin might affect other immune cells

(e.g., natural killer cells and dendritic cells) warrants further investigation.

Human MDSCs comprise a heterogeneous population of myeloid cells with the ability to suppress immune responses that have been poorly characterized (2, 41–43). We have previously reported that a distinct fraction among both PMN-($CD14^-CD11b^+$) and M-MDSCs ($CD14^+CD11b^+$) coexpresses functional CD39/CD73, linking their immunosuppressive and chemoprotective effects to disease progression in patients with non–small cell lung cancer (23). In line with results, we found that expression and enzymatic activity of CD39/CD73 on MDSCs inhibit $CD8^+$ T-cell immunity similarly in ovarian cancer patients, indicating the importance of CD39/CD73 in MDSC-mediated immunosuppression is not limited to a specific type of cancer.

Although the mechanisms of regulation of CD39/CD73 expression on human MDSCs are largely unknown, the present study discovers a direct connection between metformin and the CD39/CD73-mediated adenosinergic effect to reverse MDSC's suppressive function. Metformin as the most widely used antidiabetic drug emerges recently as an anticancer agent via AMPK activation that is a major energy sensor of the energetic status of the cell, which may affect the metabolism of adenylates including ATP, ADP, and AMP. This led us to identify possible cross-talk between metformin-induced AMPK activation and adenosinergic effect in MDSCs. In this study, we provide the new evidence that metformin is able to limit adenosine generation from ATP, ADP, and AMP through reducing the MDSC expression and ectoenzyme activity of CD39/CD73. In an effort to reveal the molecular basis for metformin-mediated inhibitory effect on MDSC activity, our data support a model in which metformin inhibits expression and activity of CD39/CD73 through activation of AMPKα and inhibition of the HIF1α pathway to impair MDSC's immunosuppressive activity, thereby improving antitumor T-cell immune responses. Consistent with this notion, AMPK downstream-activated signaling pathways were found to be implicated in the maturation of BM cells to MDSCs (44). Furthermore, metformin-mediated AMPK activation also inhibited HIF1α expression in cancer cells (45–47). However, the role of AMPK activation in reducing HIF1α expression seems to depend on the cell type. For example, hypoxia induces HIF1 expression in mouse embryonic fibroblasts independent of AMPK (48). Tumor-infiltrating T cells from metformin-treated animals had similar levels of HIF1α, even though they experienced less hypoxia. Previous studies reported the role of HIF1α in regulating function and differentiation of MDSCs in the tumor microenvironment (49–51). Our present data thus build on this platform, suggesting that metformin may limit the function and fate of MDSCs in tumor-bearing hosts by orchestrating the CD39/CD73-dependent adenosinergic effect via the AMPK/HIF1α pathway.

Depletion of MDSCs or inhibiting MDSCs function mitigates cancer progression (52, 53). Our results indicate that MDSCs are likely one primary cellular target of metformin, consistent with previous results showing a selective, inhibitory effect of phenformin (a close analog of metformin) on MDSC-driven immunosuppression (54). Our data add to an increasing number of reports (22, 55–57) suggesting the immunomodulatory effects of chemopreventive reagents on MDSCs as adjuvants for cancer therapy. Along these lines, metformin may serve as one of the potentiators of antitumor immunity. Thus, we hypothesize that many forms of immunotherapy that aim to act by reinvigorating T cells at the tumor site will be improved through modulation of this aspect of the microenvironment. This is supported by a report demonstrating improved intratumoral T-cell function and tumor clearance by combination of metformin with PD-1 checkpoint blockade in mouse tumor models (58). However, future studies will be required to understand how checkpoint blockade, stimulatory agonistic antibody therapy, or adoptive cell therapy might be improved by metformin treatment.

In this study, we highlight a new application for metformin as a potent immunomodulatory agent, which overcomes a major mechanism of tumor immune evasion by targeting CD39/CD73 on MDSCs. These data broaden our understanding about the action of metformin in cancer treatment and provide a rational basis for future clinical testing of administration of metformin in combination with cancer immunotherapeutics.

Disclosure of Potential Conflicts of Interest

No potential conflicts of interest were disclosed.

Authors' Contributions

Conception and design: L. Li, L. Wang, J. Li, Z. Fan, J.J. Yu, J. Zhao, B. Zhang, Y. Zhang

Development of methodology: L. Yang, C. Zhang, D. Yue, F. Li, X. Chen, D. Wang, Z. Sun, B. Zhang

Acquisition of data (provided animals, acquired and managed patients, provided facilities, etc.): L. Li, J. Li, Z. Zhang, C. Zhang, D. Yue, G. Qin, Y. Ping, Q. Gao, X. Zhao, W. Xue

Analysis and interpretation of data (e.g., statistical analysis, biostatistics, computational analysis): L. Li, J. Li, Z. Zhang, G. Qin, T. Zhang, F. Li, Y. Ping, D. Wang, Q. He, L. Huang, Z. Sun, J. Lu, J.J. Yu, B. Zhang

Writing, review, and/or revision of the manuscript: L. Li, J. Li, J. Lu, J.J. Yu, B. Zhang, Y. Zhang

Administrative, technical, or material support (i.e., reporting or organizing data, constructing databases): L. Wang, Z. Fan, L. Yang, G. Qin, T. Zhang, X. Chen, D. Wang, Q. Gao, Q. He, H. Li, J. Huang, X. Zhao, W. Xue, Z. Sun, Y. Zhang

Study supervision: L. Wang, F. Li, X. Chen, L. Huang, H. Li, J. Huang, X. Zhao, J. Zhao, B. Zhang, Y. Zhang

Acknowledgments

This study was supported by R01 grant from the NIH (CA149669 and CA208354), Research Pilot Study Award from the Marsha Rivkin Center for Ovarian Cancer Research, the National Natural Science Foundation of China (Grant Nos. 81171985 and 81603122), Research Grant from the Ministry of Public Health (No. 20110110001), the Basic and Advanced Technology Research Foundation from Science and Technology Department of Henan Province (Grant Nos. 112300410153 and 122300410155), Funds for Creative Research Team of Henan Province, Creative Research Team of Higher Education of Henan Province, and the Innovation Team of the First Affiliated Hospital of Zhengzhou University.

The costs of publication of this article were defrayed in part by the payment of page charges. This article must therefore be hereby marked *advertisement* in accordance with 18 U.S.C. Section 1734 solely to indicate this fact.

Received August 28, 2017; revised December 18, 2017; accepted January 23, 2018; published OnlineFirst January 26, 2018.

References

1. Gabrilovich DI, Nagaraj S. Myeloid-derived suppressor cells as regulators of the immune system. Nat Rev Immunol 2009;9:162–74.
2. Filipazzi P, Huber V, Rivoltini L. Phenotype, function and clinical implications of myeloid-derived suppressor cells in cancer patients. Cancer Immunol Immunother 2012;61:255–63.
3. Ostrand-Rosenberg S. Myeloid-derived suppressor cells: more mechanisms for inhibiting antitumor immunity. Cancer Immunol Immunother 2010; 59:1593–600.
4. Ancona C, Badaloni C, Mataloni F, Bolignano A, Bucci S, Cesaroni G, et al. Mortality and morbidity in a population exposed to multiple sources of air pollution: a retrospective cohort study using air dispersion models. Environ Res 2015;137:467–74.
5. Zou W. Regulatory T cells, tumour immunity and immunotherapy. Nat Rev Immunol 2006;6:295–307.
6. Ostrand-Rosenberg S, Sinha P. Myeloid-derived suppressor cells: linking inflammation and cancer. J Immunol 2009;182:4499–506.
7. Raychaudhuri B, Rayman P, Huang P, Grabowski M, Hambardzumyan D, Finke JH, et al. Myeloid derived suppressor cell infiltration of murine and human gliomas is associated with reduction of tumor infiltrating lymphocytes. J Neurooncol 2015;122:293–301.
8. Favaloro J, Liyadipitiya T, Brown R, Yang S, Suen H, Woodland N, et al. Myeloid derived suppressor cells are numerically, functionally and phenotypically different in patients with multiple myeloma. Leuk Lymphoma 2014;55:2893–900.
9. Horinaka A, Sakurai D, Ihara F, Makita Y, Kunii N, Motohashi S, et al. Invariant NKT cells are resistant to circulating CD15(+) myeloid-derived suppressor cells in patients with head and neck cancer. Cancer Sci 2016;107:207–16.
10. Parker KH, Beury DW, Ostrand-Rosenberg S. Myeloid-derived suppressor cells: critical cells driving immune suppression in the tumor microenvironment. Adv Cancer Res 2015;128:95–139.
11. Kumar V, Patel S, Tcyganov E, Gabrilovich DI. The nature of myeloid-derived suppressor cells in the tumor microenvironment. Trends Immunol 2016;37:208–20.
12. Munn DH, Bronte V. Immune suppressive mechanisms in the tumor microenvironment. Curr Opin Immunol 2016;39:1–6.
13. Tobin RP, Davis D, Jordan KR, McCarter MD. The clinical evidence for targeting human myeloid-derived suppressor cells in cancer patients. J Leukoc Biol 2017;102:381–91.
14. Najjar YG, Finke JH. Clinical perspectives on targeting of myeloid derived suppressor cells in the treatment of cancer. Front Oncol 2013;3:49.
15. Wesolowski R, Markowitz J, Carson WE 3rd. Myeloid derived suppressor cells - a new therapeutic target in the treatment of cancer. J Immunothera Cancer 2013;1:10.
16. Hatfield SM, Sitkovsky M. A2A adenosine receptor antagonists to weaken the hypoxia-HIF-1alpha driven immunosuppression and improve immunotherapies of cancer. Curr Opin Pharmacol 2016;29:90–6.
17. Young A, Mittal D, Stagg J, Smyth MJ. Targeting cancer-derived adenosine: new therapeutic approaches. Cancer Discov 2014;4:879–88.
18. Zhang B. CD73: a novel target for cancer immunotherapy. Cancer Res 2010;70:6407–11.
19. Allard B, Longhi MS, Robson SC, Stagg J. The ectonucleotidases CD39 and CD73: novel checkpoint inhibitor targets. Immunol Rev 2017;276: 121–44.
20. Beavis PA, Stagg J, Darcy PK, Smyth MJ. CD73: a potent suppressor of antitumor immune responses. Trends Immunol 2012;33:231–7.
21. Zhang B. Opportunities and challenges for anti-CD73 cancer therapy. Immunotherapy 2012;4:861–5.
22. Ye C, Geng Z, Dominguez D, Chen S, Fan J, Qin L, et al. Targeting ornithine decarboxylase by alpha-difluoromethylornithine inhibits tumor growth by impairing myeloid-derived suppressor cells. J Immunol 2016;196:915–23.
23. Li J, Wang L, Chen X, Li L, Li Y, Ping Y, et al. CD39/CD73 upregulation on myeloid-derived suppressor cells via TGF-beta-mTOR-HIF-1 signaling in patients with non-small cell lung cancer. Oncoimmunology 2017;6: e1320011.
24. Bodmer M, Meier C, Krahenbuhl S, Jick SS, Meier CR. Long-term metformin use is associated with decreased risk of breast cancer. Diabetes Care 2010;33:1304–8.
25. Evans JM, Donnelly LA, Emslie-Smith AM, Alessi DR, Morris AD. Metformin and reduced risk of cancer in diabetic patients. BMJ 2005;330:1304–5.
26. Daugan M, Dufay Wojcicki A, d'Hayer B, Boudy V. Metformin: an anti-diabetic drug to fight cancer. Pharmacol Res 2016;113:675–85.
27. Foretz M, Guigas B, Bertrand L, Pollak M, Viollet B. Metformin: from mechanisms of action to therapies. Cell Metab 2014;20:953–66.
28. Pernicova I, Korbonits M. Metformin–mode of action and clinical implications for diabetes and cancer. Nat Rev Endocrinol 2014;10:143–56.
29. Synnestvedt K, Furuta GT, Comerford KM, Louis N, Karhausen J, Eltzschig HK, et al. Ecto-5′-nucleotidase (CD73) regulation by hypoxia-inducible factor-1 mediates permeability changes in intestinal epithelia. J Clin Invest 2002;110:993–1002.
30. Bronte V, Brandau S, Chen SH, Colombo MP, Frey AB, Greten TF, et al. Recommendations for myeloid-derived suppressor cell nomenclature and characterization standards. Nat Commun 2016;7:12150.
31. Feng PH, Lee KY, Chang YL, Chan YF, Kuo LW, Lin TY, et al. CD14(+) S100A9(+) monocytic myeloid-derived suppressor cells and their clinical relevance in non-small cell lung cancer. Am J Respir Crit Care Med 2012;186:1025–36.
32. Ryzhov S, Novitskiy SV, Goldstein AE, Biktasova A, Blackburn MR, Biaggioni I, et al. Adenosinergic regulation of the expansion and immunosuppressive activity of CD11b+Gr1+ cells. J Immunol 2011;187:6120–9.
33. Wu T, Zhao Y, Wang H, Li Y, Shao L, Wang R, et al. mTOR masters monocytic myeloid-derived suppressor cells in mice with allografts or tumors. Sci Rep 2016;6:20250.
34. Schott S, Bierhaus A, Schuetz F, Beckhove P, Schneeweiss A, Sohn C, et al. Therapeutic effects of metformin in breast cancer: involvement of the immune system? Cancer Immunol Immunothera 2011;60:1221–5.
35. Pearce EL, Walsh MC, Cejas PJ, Harms GM, Shen H, Wang LS, et al. Enhancing CD8 T-cell memory by modulating fatty acid metabolism. Nature 2009;460:103–7.
36. Blagih J, Coulombe F, Vincent EE, Dupuy F, Galicia-Vazquez G, Yurchenko E, et al. The energy sensor AMPK regulates T cell metabolic adaptation and effector responses in vivo. Immunity 2015;42:41–54.
37. Eikawa S, Nishida M, Mizukami S, Yamazaki C, Nakayama E, Udono H. Immune-mediated antitumor effect by type 2 diabetes drug, metformin. PNAS 2015;112:1809–14.
38. Nath N, Khan M, Paintlia MK, Singh I, Hoda MN, Giri S. Metformin attenuated the autoimmune disease of the central nervous system in animal models of multiple sclerosis. J Immunol 2009;182:8005–14.
39. Park MJ, Lee SY, Moon SJ, Son HJ, Lee SH, Kim EK, et al. Metformin attenuates graft-versus-host disease via restricting mammalian target of rapamycin/signal transducer and activator of transcription 3 and promoting adenosine monophosphate-activated protein kinase-autophagy for the balance between T helper 17 and Tregs. Translat Res 2016;173: 115–30.
40. Zhao D, Long XD, Lu TF, Wang T, Zhang WW, Liu YX, et al. Metformin decreases IL-22 secretion to suppress tumor growth in an orthotopic mouse model of hepatocellular carcinoma. Int J Cancer 2015;136:2556–65.
41. Gabrilovich DI, Ostrand-Rosenberg S, Bronte V. Coordinated regulation of myeloid cells by tumours. Nat Rev Immunol 2012;12:253–68.
42. Peranzoni E, Zilio S, Marigo I, Dolcetti L, Zanovello P, Mandruzzato S, et al. Myeloid-derived suppressor cell heterogeneity and subset definition. Curr Opin Immunol 2010;22:238–44.
43. Solito S, Marigo I, Pinton L, Damuzzo V, Mandruzzato S, Bronte V. Myeloid-derived suppressor cell heterogeneity in human cancers. Ann N Y Acad Sci 2014;1319:47–65.
44. Hammami I, Chen J, Murschel F, Bronte V, De Crescenzo G, Jolicoeur M. Immunosuppressive activity enhances central carbon metabolism and bioenergetics in myeloid-derived suppressor cells in vitro models. BMC Cell Biol 2012;13:18.
45. Qi X, Xu W, Xie J, Wang Y, Han S, Wei Z, et al. Metformin sensitizes the response of oral squamous cell carcinoma to cisplatin treatment through inhibition of NF-kappaB/HIF-1alpha signal axis. Sci Rep 2016;6:35788.
46. Feng T, Li L, Ling S, Fan N, Fang M, Zhang H, et al. Metformin enhances radiation response of ECa109 cells through activation of ATM and AMPK. Biom Pharmacother 2015;69:260–6.
47. Lee M, Hwang JT, Lee HJ, Jung SN, Kang I, Chi SG, et al. AMP-activated protein kinase activity is critical for hypoxia-inducible factor-1 transcriptional activity and its target gene expression under hypoxic conditions in DU145 cells. J Biol Chem 2003;278:39653–61.

48. Emerling BM, Viollet B, Tormos KV, Chandel NS. Compound C inhibits hypoxic activation of HIF-1 independent of AMPK. FEBS Lett 2007;581: 5727–31.
49. Noman MZ, Desantis G, Janji B, Hasmim M, Karray S, Dessen P, et al. PD-L1 is a novel direct target of HIF-1alpha, and its blockade under hypoxia enhanced MDSC-mediated T cell activation. J Exp Med 2014; 211:781–90.
50. Liu G, Bi Y, Shen B, Yang H, Zhang Y, Wang X, et al. SIRT1 limits the function and fate of myeloid-derived suppressor cells in tumors by orchestrating HIF-1alpha-dependent glycolysis. Cancer Res 2014;74: 727–37.
51. Corzo CA, Condamine T, Lu L, Cotter MJ, Youn JI, Cheng P, et al. HIF-1alpha regulates function and differentiation of myeloid-derived suppressor cells in the tumor microenvironment. J Exp Med 2010;207: 2439–53.
52. Iclozan C, Antonia S, Chiappori A, Chen DT, Gabrilovich D. Therapeutic regulation of myeloid-derived suppressor cells and immune response to cancer vaccine in patients with extensive stage small cell lung cancer. Cancer Immunol Immunothera 2013;62:909–18.
53. Highfill SL, Cui Y, Giles AJ, Smith JP, Zhang H, Morse E, et al. Disruption of CXCR2-mediated MDSC tumor trafficking enhances anti-PD1 efficacy. Sci Transl Med 2014;6:237ra67.
54. Kim SH, Li M, Trousil S, Zhang Y, Pasca di Magliano M, Swanson KD, et al. Phenformin inhibits myeloid-derived suppressor cells and enhances the anti-tumor activity of PD-1 blockade in melanoma. J Invest Dermatol 2017;137:1740–8.
55. Kodumudi KN, Woan K, Gilvary DL, Sahakian E, Wei S, Djeu JY. A novel chemoimmunomodulating property of docetaxel: suppression of myeloid-derived suppressor cells in tumor bearers. Clin Cancer Res 2010;16:4583–94.
56. Kang TH, Knoff J, Yeh WH, Yang B, Wang C, Kim YS, et al. Treatment of tumors with vitamin E suppresses myeloid derived suppressor cells and enhances CD8+ T cell-mediated antitumor effects. PLoS One 2014;9:e103562.
57. Gupta P, Wright SE, Srivastava SK. PEITC treatment suppresses myeloid derived tumor suppressor cells to inhibit breast tumor growth. Oncoimmunology 2015;4:e981449.
58. Scharping NE, Menk AV, Whetstone RD, Zeng X, Delgoffe GM. Efficacy of PD-1 blockade is potentiated by metformin-induced reduction of tumor hypoxia. Cancer Immunol Res 2017;5:9–16.